

Structural and dynamical properties of sodium silicate melts: An investigation by molecular dynamics computer simulation

Jürgen Horbach, Walter Kob, and Kurt Binder

Institute of Physics, Johannes Gutenberg University, Staudinger Weg 7, D-55099 Mainz, Germany

Abstract

We present the results of large scale computer simulations in which we investigate the static and dynamic properties of sodium disilicate and sodium trisilicate melts. We study in detail the static properties of these systems, namely the coordination numbers, the temperature dependence of the $Q^{(n)}$ species and the static structure factor, and compare them with experiments. We show that the structure is described by a partially destroyed tetrahedral SiO_4 network and the homogeneously distributed sodium atoms which are surrounded on average by 16 silicon and other sodium atoms as nearest neighbors. We compare the diffusion of the ions in the sodium silicate systems with that in pure silica and show that it is much slower in the latter. The sodium diffusion is characterized by an activated hopping through the Si–O matrix which is frozen with respect to the movement of the sodium atoms. We identify the elementary diffusion steps for the sodium and the oxygen diffusion and find that in the case of sodium they are related to the breaking of a Na–Na bond and in the case of oxygen to that of a Si–O bond. From the self part of the van Hove correlation function we recognize that at least two successive diffusion steps of a sodium atom are spatially highly correlated with each other. With the same quantity we show that at low temperatures also the oxygen diffusion is characterized by activated hopping events.

I. INTRODUCTION

Silicate melts and glasses are an important class of materials in very different fields, e.g. in geosciences (since silicates are geologically the most relevant materials) and in technology (windows, containers, and optical fibers). From a physical point of view it is a very challenging task to understand the properties of these materials on a microscopic level, and in the last twenty years many studies on different systems have shown that molecular dynamics computer simulations are a very appropriate tool for this purpose (Angell *et al.*, 1981, Balucani and Zoppi, 1994, Kob, 1999). The main advantage of such simulations is that they give access to the whole microscopic information in form of the particle trajectories which of course cannot be determined in real experiments.

In pure silica (SiO_2) the structure is that of a disordered tetrahedral network in which SiO_4 tetrahedra are connected via the oxygens at the edges. In a recent simulation (Horbach and Kob, 1999a) we have studied in detail the statics and dynamics of pure silica. In the present paper we investigate the statics and dynamics of melts in which the network modifier sodium is added to a silica melt. In particular two sodium silicate systems are discussed, namely sodium disilicate ($\text{Na}_2\text{Si}_2\text{O}_5$) and sodium trisilicate ($\text{Na}_2\text{Si}_3\text{O}_7$) to which will be referred to NS2 and NS3, respectively.

In recent years several authors found, by using the potential proposed by Vessal *et al.* (1989) that, e.g., NS2 is characterized by a microsegregation in which the sodium atoms form clusters of a few atoms between bridged SiO_4 units (Vessal *et al.*, 1992, Smith *et al.*, 1995, Cormack and Cao, 1997). This result is somewhat surprising because in experiments one observes a phase separation between Na_2O and SiO_2 at lower temperatures and more likely in sodium silicates with a higher SiO_2 concentration (Mazurin *et al.*, 1970, Haller *et al.*, 1974). In order to see whether microsegregation is also reproduced with a different model from the one of Vessal *et al.* we have performed our simulations with a different potential (discussed below).

Up to now the dynamics of systems like alkali silicates was investigated by studying only the dynamics of the alkali atoms which, at lower temperatures, is much faster than that of the silicon and oxygen atoms. In this paper we therefore present the results for the diffusion dynamics of all components in NS2 and NS3 as well as the microscopic mechanism of diffusion in these systems.

II. MODEL AND DETAILS OF THE SIMULATIONS

In a classical molecular dynamics computer simulation one solves numerically Newton's equations of motion for a many particle system. If quantum mechanical effects can be neglected such simulations are able to give in principle a realistic description of any molecular system. The determining factor of how well the properties of a real material are reproduced by a MD simulation is the potential with which the interaction between the atoms is described. The model potential we use to compute the interaction between the ions in sodium silicates is the one proposed by Kramer *et al.* (1991) which is a generalization of the so called BKS potential (van Beest *et al.*, 1990) for pure silica. It has the following functional form:

$$\phi(r) = \frac{q_\alpha q_\beta e^2}{r} + A_{\alpha\beta} \exp(-B_{\alpha\beta} r) - \frac{C_{\alpha\beta}}{r^6} \quad \alpha, \beta \in [\text{Si}, \text{Na}, \text{O}]. \quad (1)$$

Here r is the distance between an ion of type α and an ion of type β . The values of the parameters $A_{\alpha\beta}$, $B_{\alpha\beta}$ and $C_{\alpha\beta}$ can be found in the original publication. The potential (1) has been optimized by Kramer *et al.* for zeolites, i.e. for systems that have Al ions in addition to Si, Na and O. In that paper the authors used for silicon and oxygen the *partial* charges $q_{\text{Si}} = 2.4$ and $q_{\text{O}} = -1.2$, respectively, whereas sodium was assigned its real ion charge $q_{\text{Na}} = 1.0$. With this choice charge neutrality is not fulfilled in sodium silicate systems. To overcome this problem we introduced for the sodium ions a distance dependent charge $q(r)$ instead of q_{Na} ,

$$q(r) = \begin{cases} 0.6 \left(1 + \ln \left[C (r_c - r)^2 + 1 \right] \right) & r < r_c \\ 0.6 & r \geq r_c \end{cases} \quad (2)$$

which means that for $r \geq r_c$ charge neutrality is valid ($q(r) = 0.6$ for $r \geq r_c$). Note that $q(r)$ is continuous at r_c . We have fixed the parameters r_c and C such that the experimental mass density of NS2 and the static structure factor from a neutron scattering experiment are reproduced well. From this fitting we have obtained the values $r_c = 4.9 \text{ \AA}$ and $C = 0.0926 \text{ \AA}^{-2}$. With this choice the charge $q(r)$ crosses smoothly over from $q(r) = 1.0$ at 1.7 \AA to $q(r) = 0.6$ for $r \geq r_c$.

The simulations have been done at constant volume with the density of the system fixed to 2.37 g/cm^3 . The systems consist of 8064 and 8016 ions for NS2 and NS3, respectively. The reason for using such a relatively large system size is that, like in SiO_2 (Horbach *et al.*, 1996, Horbach *et al.*, 1999b), strong finite size effects are present in the dynamics of smaller systems which have to be avoided (Horbach and Kob, 1999c). The equations of motion were integrated with the velocity form of the Verlet algorithm and the Coulombic contributions to the potential and the forces were calculated via Ewald summation. The time step of the integration was 1.6 fs. The temperatures investigated are 4000 K, 3400 K, 3000 K, 2750 K, 2500 K, 2300 K, 2100 K, and in addition for NS2 also 1900 K. The temperature of the system was controlled by coupling it to a stochastic heat bath, i.e. by substituting periodically the velocities of the particles with the ones from a Maxwell-Boltzmann distribution with the correct temperature. After the system was equilibrated at the target temperature, we continued the run in the microcanonical ensemble, i.e. the heat bath was switched off. In order to improve the statistics we have done two independent runs at each temperature. The production runs have been up to 7.5 ns real time which corresponds to 4.5 million time steps. In the temperature range under investigation the pressure decreases monotonically from 3.8 GPa to 1.8 GPa in the case of NS3 and from 7.3 GPa to 4.1 GPa in the case of NS2. In order to make a comparison of the static structure factor for NS2 from our simulation with one from a neutron scattering experiment (see below) we have also determined the structures of the glass at $T = 300 \text{ K}$. The glass state was produced by cooling the system from equilibrated configurations at $T = 1900 \text{ K}$ with a cooling rate of $1.16 \cdot 10^{12} \text{ K/s}$. The pressure of the system at $T = 300 \text{ K}$ is 0.96 GPa.

In the following we compare the properties of NS2 and NS3 with those of pure silica which we have investigated in recent simulation. The details of the latter can be found in Horbach and Kob (1999a). We only mention here that these simulations were done also at the density 2.37 g/cm^3 in the temperature range $6100 \text{ K} \geq T \geq 2750 \text{ K}$ for a system of 8016 particles. The two production runs at the lowest temperature were over about 20 ns real time, and the pressure at this temperature is 0.9 GPa.

III. RESULTS

A. Structural properties

In order to investigate the local environment of an atom in a disordered structure, especially at high temperatures, it is useful to calculate the coordination number $z_{\alpha\beta}(r)$ which gives the number of atoms of type $\beta \in [\text{Si}, \text{Na}, \text{O}]$ surrounding an atom of type $\alpha \in [\text{Si}, \text{Na}, \text{O}]$ within a distance $r' \leq r$. Note that $z_{\alpha\beta}(r)$ is essentially the integral from $r' = 0$ to $r' = r$ over the function $4\pi r'^2 g_{\alpha\beta}(r')$, where $g_{\alpha\beta}(r)$ denotes the pair correlation function for $\alpha\beta$ correlations (Balucani and Zoppi, 1994). In Fig. 1a we show $z_{\text{Si-O}}(r)$ and $z_{\text{O-Si}}(r)$ for SiO_2

at $T = 2750$ K and for NS3 and NS2 at $T = 2100$ K. In both quantities we observe a strong increase for distances from 1.5 \AA to 1.7 \AA at which the functions reach a plateau which persists up to about 3.0 \AA . For distances $r > 3.0 \text{ \AA}$ there is no such step like behavior because of the disorder. The vertical lines in Fig. 1a at $\bar{r}_{\text{Si-O}} = 1.61 \text{ \AA}$ and $r_{\text{min}}^{\text{Si-O}} = 2.35 \text{ \AA}$ correspond to the first maximum and the first minimum in $g_{\text{SiO}}(r)$, respectively. In $z_{\text{Si-O}}(r)$ the plateau is essentially at $z = 4$ in SiO_2 as well as in the sodium silicate systems which means that most of the silicon atoms, i.e. more than 99 %, are surrounded by four oxygen atoms thus forming a tetrahedron. In the case of SiO_2 there is also a plateau essentially at $z_{\text{O-Si}} = 2$ in the same r interval. Therefore, in this system most of the the oxygen atoms are bridging oxygens between two tetrahedra, and thus the system seems to form a perfect disordered tetrahedral network even at the relatively high temperature $T = 2750$ K. Indeed we found that at this temperature less than one percent of the silicon and oxygen atoms are defects (Horbach and Kob, 1999a). For NS3 and NS2 a plateau is formed at $z_{\text{O-Si}} = 1.71$ and $z_{\text{O-Si}} = 1.6$, respectively. This is due to the fact that only a part of the oxygen atoms are bridging oxygens, namely 68.5 % in the case of NS2 and 71.3 % in the case of NS3. Most of the other oxygen atoms form dangling bonds with one silicon neighbor (28.4 % in NS2 and 22.7 % in NS3 at $r_{\text{min}}^{\text{Si-O}}$) or they are not nearest neighbors of silicon atoms (3.1 % in NS2 and 6.0 % in NS3 at $r_{\text{min}}^{\text{Si-O}}$). The local environment of the sodium atoms is characterized by $z_{\text{Na-O}}(r)$, $z_{\text{Na-Si}}(r)$, and $z_{\text{Na-Na}}(r)$ in Fig. 1b. In these quantities there is no step like behavior also at small distances. At $r_{\text{min}}^{\text{Na-O}}$, which is approximately at $r = 3.0 \text{ \AA}$ for NS3 and NS2, the apparent coordination number $z = 4.2$ is too small in comparison with X-ray experiments from which one would expect a value between 5 and 6 (see Brown *et al.*, 1995, and references therein). Also $\bar{r}_{\text{Na-O}} = 2.2 \text{ \AA}$ is too small in comparison with the values found in X-ray experiments which are between 2.3 \AA and 2.6 \AA . We recognize in Fig. 1b that in the case of NS2 the functions $z_{\text{Na-Na}}(r)$ and $z_{\text{Na-Si}}(r)$ are relatively close to each other for $r \leq r_{\text{min}}^{\text{Na-Na}}, r_{\text{min}}^{\text{Na-Si}} \approx 5.1 \text{ \AA}$. So at $r = r_{\text{min}}^{\text{Na-Na}}$ and $r = r_{\text{min}}^{\text{Na-Si}}$ the apparent coordination numbers are $z_{\text{Na-Na}} = 7.8$ and $z_{\text{Na-Si}} = 8.6$, respectively, i.e., are quite similar. In contrast to that, the coordination numbers in NS3 at $r = r_{\text{min}}^{\text{Na-Na}}$ and $r = r_{\text{min}}^{\text{Na-Si}}$ are $z_{\text{Na-Na}} = 5.8$ and $z_{\text{Na-Si}}(r) = 9.8$, respectively, which means that there is a substitution effect in NS3 such that more silicon atoms are on average in the neighborhood of an sodium atom than in NS2 because there are less sodium atoms in NS3. Therefore, in NS2 as well as in NS3 every sodium atom has on average about 16 silicon and sodium atoms in its neighborhood.

The structure of NS2 and NS3 can be studied in more detail by looking at the so called $Q^{(n)}$ species which can be determined experimentally by NMR (Stebbins, 1995) and by Raman spectroscopy (McMillan and Wolf, 1995). $Q^{(n)}$ is defined as the fraction of SiO_4 tetrahedra with n bridging oxygens in the system. In Fig. 1a we have seen that these structural elements are very well defined also at temperatures as high as $T = 2100$ K. From Fig. 2 we recognize that at $T = 2100$ K there is essentially a ternary distribution of $Q^{(2)}$, $Q^{(3)}$, and $Q^{(4)}$ both in NS2 and in NS3. At higher temperatures there is also a significant contribution of silicon defects, i.e. three- and five-fold coordinated silicon atoms (denoted as rest in the figure), and of $Q^{(1)}$ species. For $T \leq 3200$ K the curves for $Q^{(2)}$ are well described by Arrhenius laws $f(T) \propto \exp(E_A/T)$ (bold solid lines in Fig. 2) with activation energies $E_A = 5441$ K and $E_A = 6431$ K for NS2 and NS3, respectively. If we extrapolate these Arrhenius laws to low temperatures we recognize from Fig. 2 that the $Q^{(2)}$ species essentially disappear slightly above the experimental glass transition temperatures $T_{\text{g,exp}}$ for

NS2 and NS3, which are at 740 K and 760 K (Knoche *et al.*, 1994), respectively. Therefore, if we would be able to equilibrate our systems down to $T_{g,\text{exp}}$ we would expect a binary distribution of $Q^{(3)}$ and $Q^{(4)}$ species in the glass state of NS2 and NS3. Also included in Fig. 2 is the $Q^{(n)}$ species distribution for NS2 at $T = 300$ K which we have calculated from the configurations which we have produced by cooling down the system from $T = 1900$ K to $T = 300$ K with a cooling rate of 10^{12} K/s. We recognize from the data that the $Q^{(n)}$ species distribution essentially coincides at $T = 300$ K with the one at $T = 2100$ K, which is due to the fact that the liquid structure at the latter temperature has just been frozen in. If we extrapolate the data from 2100 K to lower temperatures allowing further relaxation we would expect about 45 % $Q^{(3)}$ and 55 % $Q^{(4)}$ in the case of NS3 and about 40 % $Q^{(3)}$ and 60 % $Q^{(4)}$ in the case of NS2 at $T_{g,\text{exp}}$. In contrast to these values one finds in NMR and Raman experiments 60 % $Q^{(3)}$ and 40 % $Q^{(4)}$ in the case of NS3 and 92 % $Q^{(3)}$ and 8 % $Q^{(4)}$ in the case of NS2 (Stebbins, 1988, Mysen and Frantz, 1992, Sprenger *et al.*, 1992, Knoche, 1993). Thus our simple model is not able to describe the $Q^{(n)}$ species reliably. The reason for this is probably that our model gives a slightly wrong coordination function $z_{\text{Na-O}}(r)$ as we have mentioned before.

So far we have looked at the local environment of the atoms. In order to investigate the structure on a larger length scale useful quantities are the partial static structure factors,

$$S_{\alpha\beta}(q) = \frac{f_{\alpha\beta}}{N} \sum_{l=1}^{N_\alpha} \sum_{m=1}^{N_\beta} \langle \exp(i\mathbf{q} \cdot (\mathbf{r}_l - \mathbf{r}_m)) \rangle, \quad (3)$$

depending on the magnitude of the wave-vector \mathbf{q} . The factor $f_{\alpha\beta}$ is equal to 0.5 for $\alpha \neq \beta$ and equal to 1.0 for $\alpha = \beta$. As examples Figs. 3a and 3b show $S_{\text{OO}}(q)$ and $S_{\text{NaNa}}(q)$ at the temperatures $T = 4000$ K and $T = 2100$ K for NS2 and NS3, respectively. The peak at 2.8 \AA^{-1} in $S_{\text{OO}}(q)$ for NS2 and NS3 corresponds to the length scale $2\pi/2.8 \text{ \AA}^{-1} = 2.24 \text{ \AA}$ which is approximately the period of the oscillations in $g_{\text{OO}}(r)$. In the same way the peak at 2.1 \AA^{-1} in $S_{\text{NaNa}}(q)$ is due to the period of oscillations in $g_{\text{NaNa}}(r)$. Moreover, the temperature dependence we observe for the peaks at 2.8 \AA^{-1} and 2.1 \AA^{-1} is relatively weak. At $T = 2100$ K a peak is visible at 1.7 \AA^{-1} in $S_{\text{OO}}(q)$ for NS2 and NS3, which is the so called first sharp diffraction peak (FSDP). This feature arises from the tetrahedral network structure since the length scale which corresponds to it, i.e. $2\pi/1.7 \text{ \AA}^{-1} = 3.7 \text{ \AA}$, is approximately the spatial extent of two connected SiO_4 tetrahedra. Only a shoulder can be identified in $S_{\text{OO}}(q)$ for $T = 4000$ K at the position of the FSDP because the network structure is less pronounced than at $T = 2100$ K. In agreement with the aforementioned interpretation of the FSDP this feature is absent in the Na–Na correlations. We note that this holds also for the Na–O and Si–Na correlations. We see therefore that the structure in NS2 is characterized by a partially destroyed tetrahedral network, and that on the other hand there are the sodium atoms which are homogeneously distributed in the system having on average 16 sodium and silicon neighbors. We would therefore expect that there is a characteristic length scale of regions where the network is destroyed and where the sodium atoms are located. This explains the peak at $q = 0.95 \text{ \AA}^{-1}$ in the $S_{\alpha\beta}(q)$ corresponding to a length scale $2\pi/0.95 \text{ \AA}^{-1} = 6.6 \text{ \AA}$ which is approximately two times the mean distance of nearest Na–Na or Na–Si neighbors. We mention that this peak is also present in the Si–Si, Si–O, Si–Na, and Na–O correlations. We emphasize that no evidence for a microsegregation

is found in the partial structure factors both for NS2 and for NS3, at least at the density of this study 2.37 g/cm^3 .

In order to make a comparison of the static structure factor for NS2 measured in a neutron scattering experiment by Misawa *et al.* (1980) with that from our model we have to determine $S^{\text{neu}}(q)$ which is calculated by weighting the partial structure factors from the simulation with the experimental coherent neutron scattering lengths b_α ($\alpha \in [\text{Si}, \text{Na}, \text{O}]$):

$$S^{\text{neu}}(q) = \frac{1}{\sum_\alpha N_\alpha b_\alpha^2} \sum_{\alpha\beta} b_\alpha b_\beta S_{\alpha\beta}(q). \quad (4)$$

The values for b_α are $0.4149 \cdot 10^{-12} \text{ cm}$, $0.363 \cdot 10^{-12} \text{ cm}$ and $0.5803 \cdot 10^{-12} \text{ cm}$ for silicon, sodium and oxygen, respectively. They are taken from Susman *et al.* (1991) for silicon and oxygen and from Bacon (1972) for sodium. Fig. 4 shows $S^{\text{neu}}(q)$ from the simulation and the experiment at $T = 300 \text{ K}$. We see that the overall agreement between simulation and experiment is good. For $q > 2.3 \text{ \AA}^{-1}$ the largest discrepancy is at the peak located at $q = 2.8 \text{ \AA}^{-1}$ where the simulation underestimates the experiment by approximately 15% in amplitude. Very well reproduced is the peak at $q = 1.7 \text{ \AA}^{-1}$. The peak at $q = 0.95 \text{ \AA}^{-1}$ is not present in the experimental data which might be due to the fact that this feature is less pronounced in real systems.

B. Dynamical properties

One of the simplest quantities to study the dynamics of liquids is the self diffusion constant D_α for a tagged particle of type α , which can be calculated from the mean squared displacement $\langle r_\alpha^2(t) \rangle$ via the Einstein relation,

$$D_\alpha = \lim_{t \rightarrow \infty} \frac{\langle r_\alpha^2(t) \rangle}{6t}. \quad (5)$$

The different D_α for NS2 and NS3 are shown in Fig. 5 as a function of the inverse temperature. Also included are the diffusion constants for pure silica from our recent simulation (Horbach and Kob, 1999a). For the latter system D_{Si} and D_{O} show at low temperatures the expected Arrhenius dependence, i.e. $D_\alpha \propto \exp[E_A/(k_B T)]$. The corresponding activation energies E_A are in very good agreement with the experimental values by Brébec *et al.* (1980) and Mikkelsen (1984) (given in the figure). We recognize from Fig. 5 that the dynamics in the sodium silicate melts is much faster than in SiO_2 even at the relatively high temperature $T = 2750 \text{ K}$ ($10^4/T = 3.64 \text{ K}^{-1}$) for which D_{Si} and D_{O} are about two orders of magnitude larger in NS2 and NS3 than in SiO_2 . Furthermore, we see that the sodium diffusion constants can be fitted in the whole temperature range very well with Arrhenius laws. The corresponding activation energies are $E_A = 0.93 \text{ eV}$ for NS2 and $E_A = 1.26 \text{ eV}$ for NS3. These activation energies are about 20 % to 30 % higher than those obtained from electrical conductivity measurements (Greaves and Ngai, 1995, and references therein). But this discrepancy might at least be partly due to the fact that our simulations are done at relatively high pressures. With decreasing temperature D_{Na} decouples more and more from D_{O} and D_{Si} in NS2 and NS3. Therefore, at least at low temperatures, the motion of the oxygen and silicon atoms is frozen with respect to the timescale of motion of the sodium atoms.

Experimentally the diffusion constants for oxygen and silicon have been measured by Poe *et al.* (1997) for the system $\text{Na}_2\text{Si}_4\text{O}_9$ at high temperatures and high pressures. Besides a few other combinations of temperature and pressure they determined D_{Si} and D_{O} at $T = 2800$ K and $p = 10$ GPa where they found the values $D_{\text{Si}} = 1.22 \cdot 10^5$ cm^2/s and $D_{\text{O}} = 1.53 \cdot 10^5$ cm^2/s . In order to make a comparison with these values we have done a simulation of $\text{Na}_2\text{Si}_4\text{O}_9$ for a system of 7680 particles at the density 2.9 g/cm^3 . At this density we have found at $T = 2800$ K and $p = 10.13$ GPa the diffusion constants $D_{\text{Si}} = 0.78 \cdot 10^5$ cm^2/s , $D_{\text{O}} = 1.17 \cdot 10^5$ cm^2/s , and $D_{\text{Na}} = 2.35 \cdot 10^5$ cm^2/s . Thus D_{Si} and D_{O} from our simulation underestimate the experimental data by less than 40% which is within the error bars of the experiment. Therefore it seems that our model gives a quite realistic description of the diffusion in sodium silicate melts.

In order to give insight into the microscopic mechanism which is responsible for the diffusion of the different species in NS2 and NS3 we discuss now the time dependence of the probability $P_{\alpha\beta}(t)$ that a bond between an atom of type α and an atom of type β is present at time t when it was present at time zero. For this we define two atoms as bonded if their distance from each other is less than the location of the first minimum r_{min} in the corresponding partial pair correlation function $g_{\alpha\beta}(r)$. In the following we restrict our discussion to NS2 because the conclusions which are drawn below also hold for NS3. From the functions $g_{\alpha\beta}(r)$ for NS2 we find for r_{min} the values 3.6 Å, 5.0 Å, 2.35 Å, 5.0 Å, 3.1 Å, and 3.15 Å for the Si–Si, Si–Na, Si–O, Na–Na, Na–O, and O–O correlations. As an example Fig. 6 shows $P_{\text{Na–Na}}$ for the different temperatures. First of all we recognize from this figure that a plateau is formed on an intermediate time scale which becomes more and more pronounced the lower the temperature is. This plateau is due to the fact that at $r = r_{\text{min}}$ the amplitude of $g_{\text{Na–Na}}(r)$ is equal 0.56 and not zero. Thus there are some sodium atoms which vibrate between the first and the second neighbor shell leading to the first fast decay of $P_{\text{Na–Na}}$ to the plateau value. In the long time regime of $P_{\text{Na–Na}}$, where it decays from the plateau to zero, its shape seems to be independent of temperature. This is also true for the functions $P_{\alpha\beta}(t)$ for the other correlations. For this reason it makes sense to define the lifetime $\tau_{\alpha\beta}$ of a bond between two atoms of type α and β as the time at which $P_{\alpha\beta}(t)$ has decayed to $1/e$. Indeed, if the function $P_{\text{Na–Na}}$ for the different temperatures is plotted versus the scaled time $t/\tau_{\text{Na–Na}}$ (inset of Fig. 6) one obtains one master curve in the long time regime $t/\tau_{\text{Na–Na}} > 0.1$. This master curve cannot be described by an exponential function but is well described by a Kohlrausch–Williams–Watts (KWW) function, $P(t) \propto \exp(-(t/\tau_{\text{Na–Na}})^\beta)$ with an exponent $\beta = 0.54$, which is shown in Fig. 6 in which this function is fitted to the curve for $T = 1900$ K.

The lifetimes $\tau_{\alpha\beta}$ can now be correlated with the diffusion constants by plotting different products $\tau_{\alpha\beta} \cdot D_\gamma$ versus temperature, which is done in Fig. 7. The product $\tau_{\text{Na–Na}} \cdot D_{\text{Na}}$ is essentially constant over the whole temperature range whereas $\tau_{\text{Na–O}} \cdot D_{\text{Na}}$ increases with decreasing temperature. This means that the elementary diffusion step for the sodium diffusion is related to the breaking of an Na–Na bond and not to that of an Na–O bond, although the nearest neighbor distance is smaller for Na–O ($r_{\text{Na–O}} = 2.2$ Å) than for Na–Na ($r_{\text{Na–Na}} = 3.3$ Å). We mention that an Arrhenius law holds also for $\tau_{\text{Na–O}}$ for which we have found the activation energy $E_A = 1.14$ eV. The latter can be interpreted as an effective Na–O binding energy in NS2. In NS3 $\tau_{\text{Na–O}}$ can be fitted with an Arrhenius law for $T < 3000$ K, the binding energy in this case is 1.64 eV. Also constant is the product $\tau_{\text{Si–O}} \cdot D_{\text{O}}$ which shows that the oxygen diffusion is related to the breaking of Si–O bonds. In contrast to that

$\tau_{\text{Si-O}} \cdot D_{\text{Si}}$ is only constant at high temperatures. For temperatures $T < 3000$ K this product decreases with decreasing temperature. Concerning the oxygen and silicon diffusion we have found recently that the same conclusions hold also for pure silica (Horbach and Kob, 1999a).

We have seen that the temperature dependence of D_{O} and D_{Si} for SiO_2 changes strongly with the addition of sodium atoms and, moreover, diffusion becomes much faster. In Fig. 8 we compare the behavior of the quantity $P_{\text{Si-O}}(t)$ for NS2, NS3 and SiO_2 at $T = 2750$ K. We recognize that the shape of the curves seems to be the same for the three systems. The only difference lies in the time scale which is, as expected from the behavior of the diffusion constants, about two orders of magnitudes larger for silica than the sodium silicate systems. That the shape of the curves is indeed the same for the three systems is demonstrated in the inset of Fig. 8 in which we have plotted the same data as before versus the scaled time $t/\tau_{\text{Si-O}}$. We see that the three curves fall nicely onto one master curve which can be fitted by a KWW law with exponent $\beta = 0.9$. This is an astonishing result for $P_{\text{Si-O}}(t)$ since the local environment of the oxygen atoms is very different in the sodium silicate systems from that in silica.

Further insight on how diffusion takes place in sodium silicates can be gained from the self part of the van Hove correlation function which is defined by (Balucani and Zoppi, 1994)

$$G_s^\alpha(r, t) = \frac{1}{N_\alpha} \sum_{i=1}^{N_\alpha} \langle \delta(r - |\mathbf{r}_i(t) - \mathbf{r}_i(0)|) \rangle \quad \alpha \in \{\text{Si, Na, O}\} \quad . \quad (6)$$

Thus $4\pi r^2 G_s^\alpha(r, t)$ is the probability to find a particle a distance r away from the place it was at $t = 0$. In Figs. 9a and 9b we show this probability for different times at $T = 2100$ K for sodium and oxygen, respectively. Note that we have chosen in both cases a linear-logarithmic plot. At $t = 0.6$ ps the sodium function exhibits a single peak with a shoulder around $r > 2.8$ Å. This shoulder becomes more pronounced as time goes on and at $t = 6.7$ ps there is a second peak located at a distance r which is equal to the average distance $\bar{r}_{\text{Na-Na}} = 3.3$ Å between two nearest sodium neighbors (marked with a vertical line in Fig. 9a). The first peak is still located at the same position as it was at $t = 0.6$ ps while its amplitude has decreased. Thus we can conclude from this that the sodium atoms do not diffuse in a continuous way but discontinuously in time by hopping on average over the distance $\bar{r}_{\text{Na-Na}}$. This interpretation was first given for similar features in a soft-sphere system by Roux *et al.* (1989). At $t = 45.7$ ps even a third peak has developed at $2\bar{r}_{\text{Na-Na}}$ while the first two peaks remain at the same position. This means that many sodium atoms have performed now a second diffusion step. We see from this that two successive elementary diffusion steps, each corresponding to a breaking of a Na-Na bond, are spatially highly correlated with each other. At $t = 164.5$ ps the function has lost its three peak structure but the first peak is still observable with a significant amplitude.

Whereas many of the sodium atoms have performed two elementary diffusion steps at $t = 45.7$ ps the amplitude of the first peak for oxygen (Fig. 9b) decreases only from about 1.5 to 0.8 in the time interval $0.6 \text{ ps} \leq t \leq 45.7 \text{ ps}$. In this time interval most of the oxygen atoms sit in the cage which is formed by the neighboring atoms and only rattle around in this cage. Nevertheless, in this time window a shoulder becomes more and more pronounced around the mean distance between two nearest oxygen neighbors $\bar{r}_{\text{O-O}} = 2.61$ Å. This means that also the oxygen diffusion takes place by activated hopping events. We have found the same behavior for oxygen at low temperatures in pure silica (Horbach and Kob, 1999a).

IV. SUMMARY

By using a simple pair potential we have performed large scale molecular dynamics simulations in order to investigate the dynamic properties of the two sodium silicate melts $\text{Na}_2\text{Si}_2\text{O}_5$ (NS2) and $\text{Na}_2\text{Si}_3\text{O}_7$ (NS3). The structure of these two systems can be characterized by a partially destroyed tetrahedral SiO_4 network, and a homogeneous distribution of sodium atoms which have on average about 16 sodium and silicon atoms as nearest neighbors. The regions in between the network structure introduce a new length scale which is about two times the distance of nearest Na–Na or Na–Si neighbors. This leads to a peak in the static structure factor at $q = 0.95 \text{ \AA}^{-1}$. Furthermore, we have found no evidence in the static structure factor that a microsegregation of Na_2O complexes takes place. A comparison of experimental data to the one of our computer simulation shows that the latter gives a fair description of the static properties of NS2 and NS3. We have explicitly demonstrated this by showing that the static structure factor $S^{\text{neu}}(q)$ from a neutron scattering experiment for NS2 (Misawa *et al.*, 1980) is reproduced quite well by our simulation. In contrast to our simulation this experiment exhibits no peak at $q = 0.95 \text{ \AA}^{-1}$ which might be due to the fact that this feature is less pronounced in real systems. Our simulations give not a very good description for the $Q^{(n)}$ species distribution which is perhaps due to the fact that our model underestimates the coordination number of nearest Na–O neighbors.

Nevertheless the oxygen and silicon diffusion constants for $\text{Na}_2\text{Si}_4\text{O}_9$ are in very good agreement with experimental data by Poe *et al.* (1997). In comparing the diffusion constants in NS2 and NS3 with those in silica we have recognized that the dynamics becomes much faster with the addition of the sodium atoms. Moreover, in the sodium silicates the diffusion constant for sodium decouples for decreasing temperature more and more from those of oxygen and silicon, such that at low temperatures the dynamics of the silicon and oxygen atoms is frozen in with respect to the movement of the sodium atoms. The sodium diffusion constants for NS2 and NS3 exhibit over the whole temperature range we investigate an Arrhenius behavior with activation energies around 1 eV.

We have shown that our simulation is able to give insight into the microscopic mechanism of diffusion in NS2 and NS3. From the time dependent bond probability $P_{\alpha\beta}(t)$ we determined an average lifetime $\tau_{\alpha\beta}$ of bonds between an atom of type α and an atom of type β . By correlating the lifetimes $\tau_{\alpha\beta}$ with the diffusion constants, we show that the elementary diffusion step in the case of sodium is the breaking of a Na–Na bond and in the case of oxygen that of a Si–O bond. By studying the self part of the van Hove correlation function we have demonstrated that at low temperatures the diffusion for oxygen and sodium takes place by activated hopping events over the mean distance $\bar{r}_{\text{O–O}} = 2.6 \text{ \AA}$ and $\bar{r}_{\text{Na–Na}} = 3.3 \text{ \AA}$, respectively. Moreover, we have found for the case of sodium that at least two successive diffusion steps are spatially highly correlated with each other.

Acknowledgments: We thank K.–U. Hess, D. Massiot, B. Poe, and J. Stebbins for useful discussions on this work. This work was supported by SFB 262/D1 and by the Deutsche Forschungsgemeinschaft, Schwerpunktsprogramm 1055. We thank the HLRZ Stuttgart for a generous grant of computer time on the CRAY T3E.

V. REFERENCES

- Angell, C. A., Clarke, J. H. R., and Woodcock, L. V., 1981. Interaction potentials and glass formation, a survey of computer experiments. *Adv. Chem. Phys.*, 48: 397–453.
- Bacon, G. E., 1972. *Acta Cryst. A*, 28: 357.
- Balucani, U., and Zoppi, M., 1994. *Dynamics of the Liquid State*. Clarendon Press, Oxford.
- Brébec, G., Seguin, R., Sella, C., Bevenot, J., and Martin, J. C., 1980. Diffusion du silicium dans la silice amorphe. *Acta Metall.*, 28, 327–333.
- Brown, G. E., Farges, F., Calas, G., 1995. X-Ray Scattering and X-Ray Spectroscopy Studies of Silicate Melts. *Rev. Mineral.*, 32: 317–410.
- Cormack, A. N., and Cao, Y., 1997. Molecular Dynamics Simulation of Silicate Glasses. In: B. Silvi and P. Arco (Eds.), *Modelling of Minerals and Silicated Materials*, Kluwer, Dordrecht: 227–271.
- Greaves, G. N., and Ngai, K. L., 1995. Reconciling ionic-transport properties with atomic structure in oxide glasses. *Phys. Rev. B*, 52: 6358–6380.
- Haller, W., Blackburn, D. H., and Simmons, J. H., 1974. Miscibility gaps in alkali-silicate binaries — data and thermodynamic interpretation. *J. Am. Ceram. Soc.*, 57: 120–126.
- Horbach, J., Kob, W., and Binder, K., 1996. Finite size effects in simulations of glass dynamics. *Phys. Rev. E*, 54: R5897–R5900.
- Horbach, J., and Kob, W., 1999a. Static and Dynamic Properties of a Viscous Silica Melt. *Phys. Rev. B* 60.
- Horbach, J., Kob, W., and Binder, K., 1999b. High frequency dynamics of amorphous silica. Submitted to *Phys. Rev. B*.
- Horbach, J., and Kob, W., 1999c. The Structure and Dynamics of Sodium Disilicate. Submitted to *Phil. Mag. B*.
- Knoche, R., 1993. *Temperaturabhängige Eigenschaften silikatischer Schmelzen*. Ph. D. thesis, Bayreuth: 100–109.
- Knoche, R., Dingwell, D. B., Seifert, F. A., and Webb, S. L., 1994. Non-linear properties of supercooled liquids in the system $\text{Na}_2\text{O-SiO}_2$. *Chem. Geol.*, 116: 1–16.
- Kob, W., 1999. Computer simulations of supercooled liquids and glasses. *J. Phys.: Condens. Matter*, 11: R85–R115.
- Kramer, G. J., de Man, A. J. M., and van Santen, R. A., 1991. Zeolites versus Aluminosilicate Clusters: The Validity of a Local Description. *J. Am. Chem. Soc.*, 64: 6435–6441.
- Mazurin, O. V., Kluyev, V. P., and Roskova, G. P., 1970. The influence of heat treatment on the viscosity of some phase separated glasses. *Phys. Chem. Glass.*, 11: 192–195.
- McMillan, P. F., and Wolf, G. H., 1995. Vibrational spectroscopy of silicate liquids. *Rev. Mineral.*, 32: 247–315.
- Mikkelsen, J. C., 1984. Self-diffusivity of network oxygen in vitreous SiO_2 . *Appl. Phys. Lett.*, 45: 1187–1189.

- Misawa, M., Price, D. L., and Suzuki, K., 1980. The short-range structure of alkali disilicate glasses by pulsed neutron total scattering. *J. Non-Cryst. Solids*, 37: 85–97.
- Mysen, B. O., and Frantz, J. D., 1992. Raman spectroscopy of silicate melts at magmatic temperatures: $\text{Na}_2\text{O-SiO}_2$, $\text{K}_2\text{O-SiO}_2$ and $\text{LiO}_2\text{-SiO}_2$ binary compositions in the temperature range 25–1475 °C. *Chem. Geol.*, 96: 321–332.
- Poe, B. T., McMillan, P. F., Rubie, D. C., Chakraborty, S., Yarger, J., and Diefenbacher, J., 1997. Silicon and Oxygen Self-Diffusivities in Silicate Liquids Measured to 15 Gigapascals and 2800 Kelvin. *Science*, 276: 1245–1248.
- Roux, J. N., Barrat, J. L., and Hansen, J.-P., 1989. Dynamical diagnostics for the glass transition in soft-sphere alloys. *J. Phys.: Condens. Matter*, 1: 7171–7186.
- Smith, W., Greaves, G. N., and Gillan, M. J., 1995. Computer simulation of sodium disilicate glass. *J. Chem. Phys.*, 103: 3091–3097.
- Sprenger, D., Bach, H., Meisel, W., and Gütlich, P., 1992. Discrete bond model (DBM) of binary silicate glasses derived from $^{29}\text{Si-NMR}$, Raman, and XPS measurements. In: *The Physics of Non-Crystalline Solids* (Eds.: D. L. Pye, W. C. La Course, and H. J. Stevens), 42–47.
- Stebbins, J. F., 1988. Effects of temperature and composition on silicate glass structure and dynamics: Si-29 NMR results. *J. Non-Cryst. Solids*, 106: 359–369.
- Stebbins, J. F., 1995. Dynamics and Structure of Silicate and Oxide Melts: Nuclear Magnetic Resonance Studies. *Rev. Mineral.*, 32: 191–247.
- Susman, S., Volin, K. J., Montague, D. G., and Price, D. L., 1991. Temperature dependence of the first sharp diffraction peak in vitreous silica. *Phys. Rev. B*, 43: 11076–11081.
- van Beest, B. W. H., Kramer, G. J., and van Santen, R. A., 1990. Force Fields for Silicas and Aluminophosphates Based on *Ab Initio* Calculations. *Phys. Rev. Lett.*, 64: 1955–1958.
- Vessal, B., Amini, M., Fincham, D., and Catlow, C. R. A., 1989. Water-like Melting Behavior of SiO_2 Investigated by the Molecular Dynamics Simulation Techniques. *Philos. Mag. B*, 60: 753–775.
- Vessal, B., Greaves, G. N., Marten, P. T., Chadwick, A. V., Mole, R., and Houde-Walter, S., 1992. Cation microsegregation and ionic mobility in mixed alkali glasses. *Nature*, 356: 504–506.

FIGURES

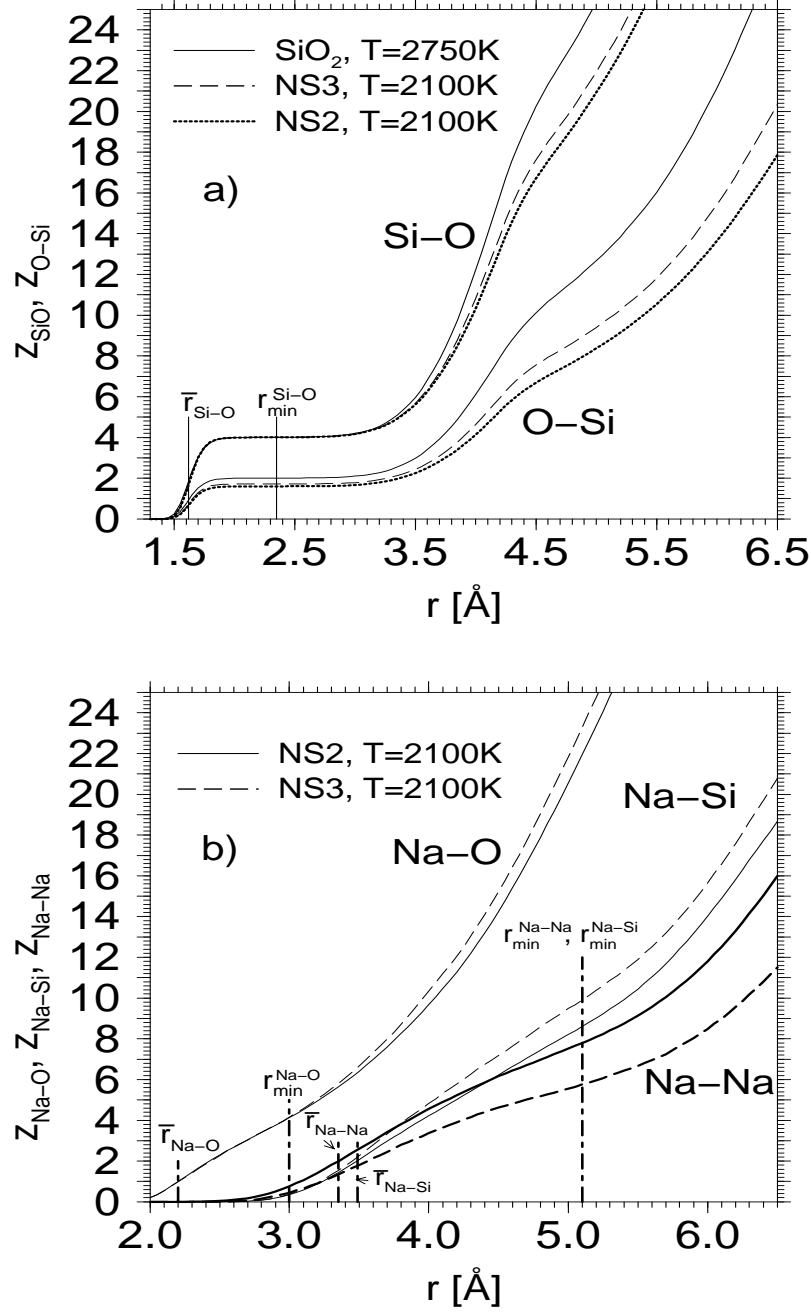


FIG. 1. Coordination numbers $z_{\alpha\beta}$ as a function of distance r at the temperature $T = 2750\text{ K}$ for SiO_2 and at $T = 2100\text{ K}$ for NS2 and NS3. a) $z_{\text{Si-O}}(r)$ and $z_{\text{O-Si}}(r)$, b) $z_{\text{Na-O}}(r)$, $z_{\text{Na-Si}}(r)$, and $z_{\text{Na-Na}}(r)$. For the explanation of the vertical lines see text.

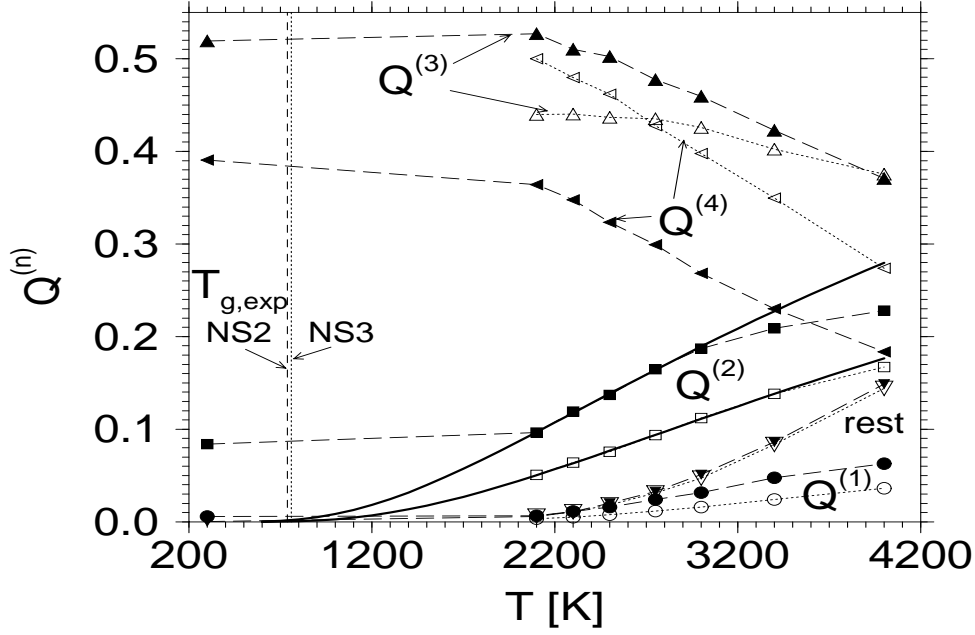


FIG. 2. Temperature dependence of the $Q^{(n)}$ species for NS2 (closed symbols) and NS3 (open symbols). The bold lines are fits with Arrhenius laws with the activation energies $E_A = 5441$ K for NS2 and $E_A = 6431$ K for NS3.

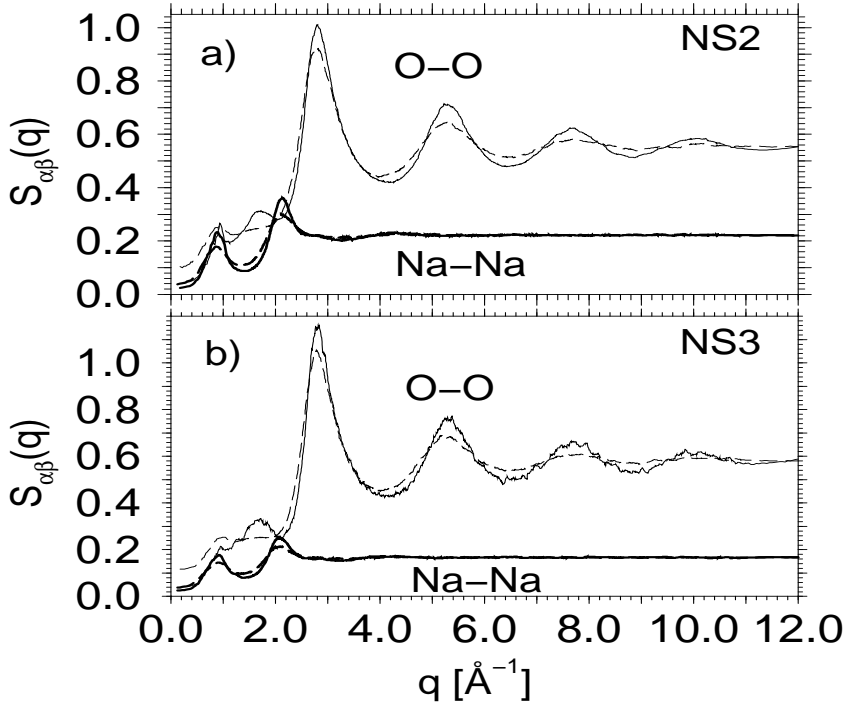


FIG. 3. Partial static structure factors $S_{OO}(q)$ (thin lines) and $S_{NaNa}(q)$ (bold lines) at the temperatures $T = 4000$ K (dashed lines) and $T = 2100$ K (solid lines), a) NS2, b) NS3.

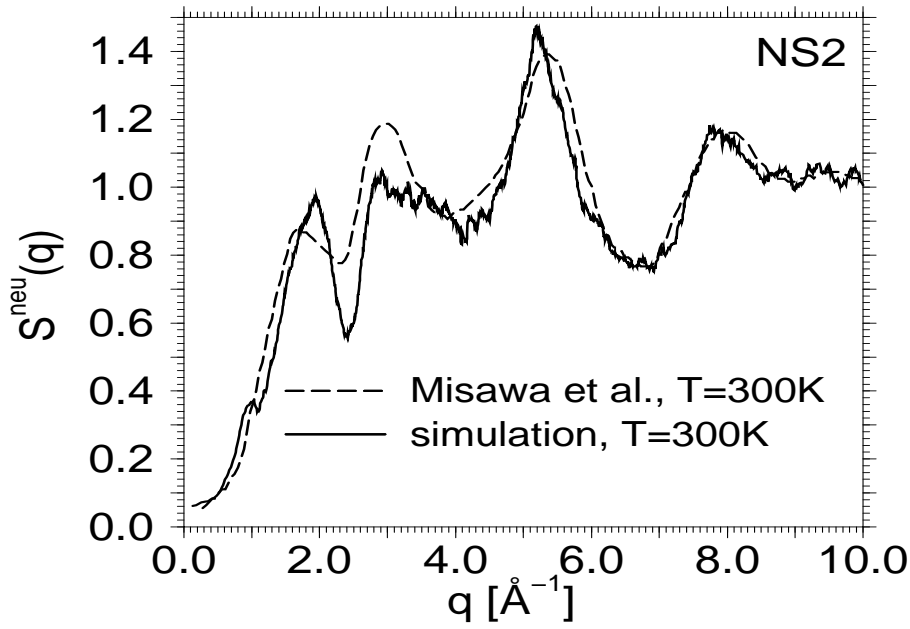


FIG. 4. Comparison of the static structure factor $S^{\text{neu}}(q)$ from our simulation (solid line) with the experimental data of Misawa *et al.* (1980) (dashed line).

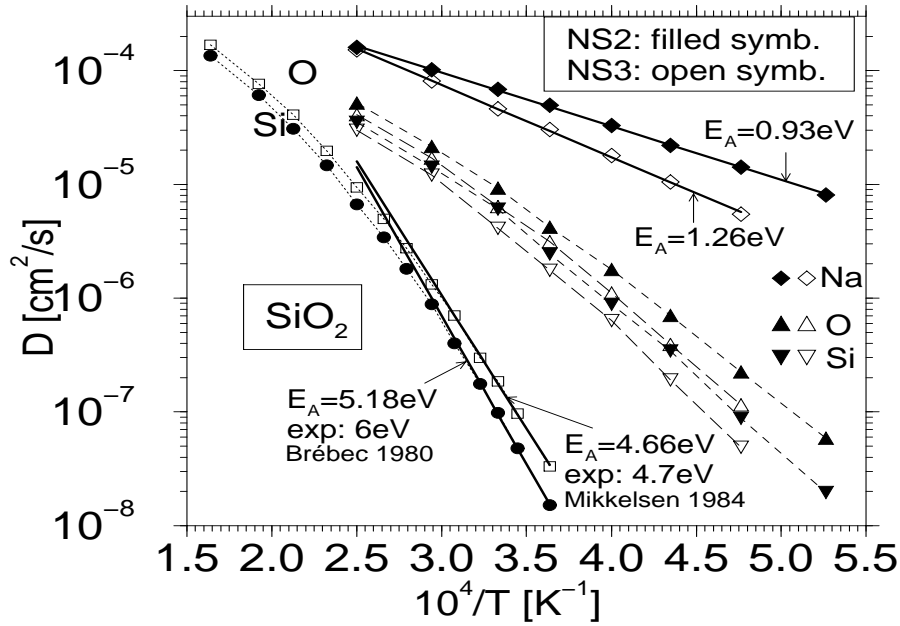


FIG. 5. The diffusion constants for SiO_2 , NS2, and NS3. The bold straight lines are fits with Arrhenius laws. The experimental values of the activation energies for silica are taken from Brébec *et al.* (1980) for silicon and from Mikkelsen (1984) for oxygen.

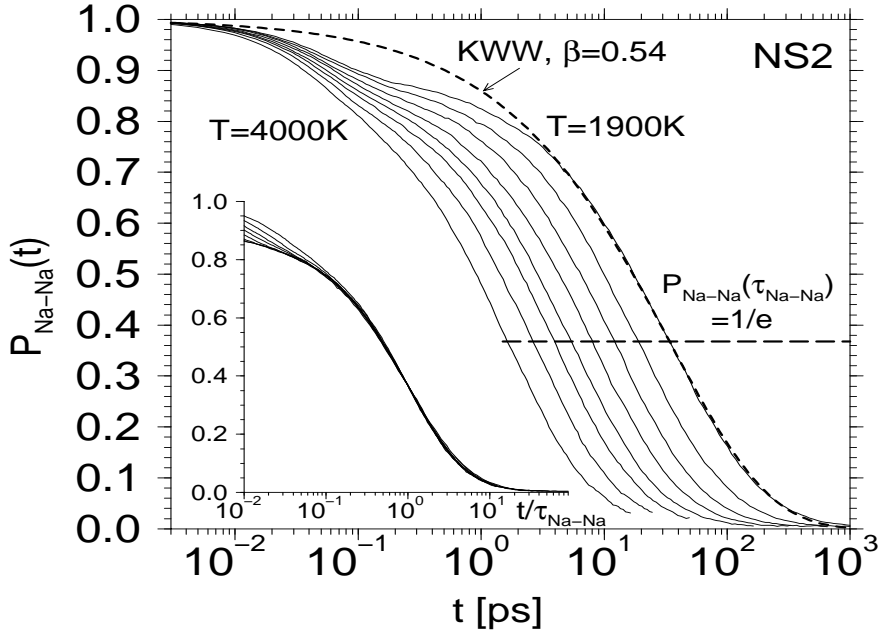


FIG. 6. Time dependence of $P_{\text{Na-Na}}$, the probability that a bond between two sodium atoms which exists at time zero is also present at time t , for all temperatures investigated. Inset: Plot of the same data versus the scaled time $t/\tau_{\text{Na-Na}}$ as a function of temperature.

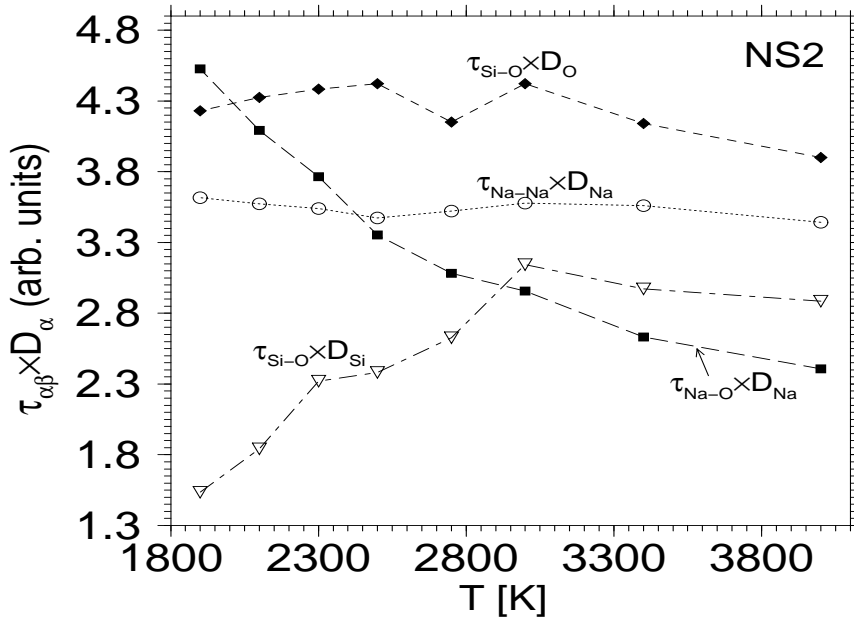


FIG. 7. The products $\tau_{\alpha\beta} \cdot D_{\alpha}$ show whether or not the diffusion constant D_{α} is correlated with the lifetime of a bond $\tau_{\alpha\beta}$.

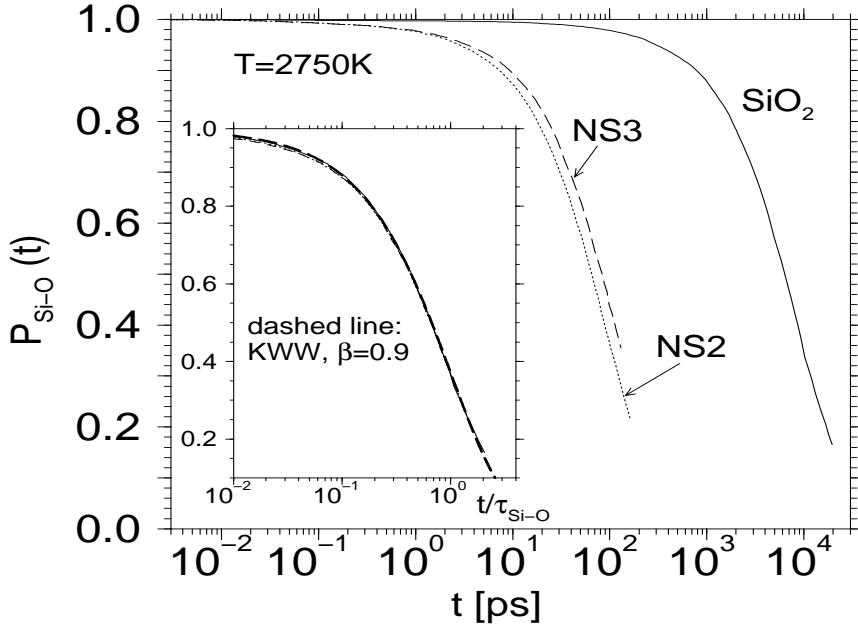


FIG. 8. $P_{\text{Si-O}}(t)$ for NS2, NS3, and SiO_2 at $T = 2750$ K. Inset: Plot of the same data versus the scaled time $t/\tau_{\text{Si-O}}$.

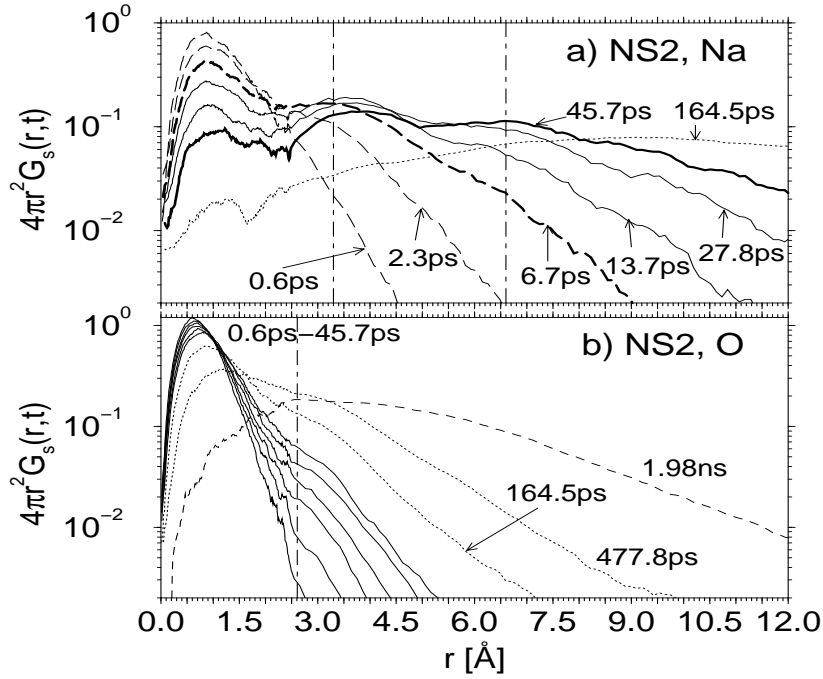


FIG. 9. Space- and time-dependence of the self part of the van Hove correlation function for NS2 at $T = 2100$ K in a linear-logarithmic plot, a) for sodium atoms, b) for oxygen atoms. The vertical lines correspond to $\bar{r}_{\text{Na-Na}} = 3.3$ Å and $2\bar{r}_{\text{Na-Na}}$ in a) and $\bar{r}_{\text{O-O}} = 2.61$ Å in b).